2015 International Symposium on Wireless Communication Systems (ISWCS), 25-28 Aug. 2015

Implementation, Validation and Application of the 3GPP 3D MIMO Channel Model in Open Source Simulation Tools

Fjolla Ademaj, Martin Taranetz, Markus Rupp

Vienna University of Technology, Institute of Telecommunications
Gusshausstrasse 25/389, A-1040 Vienna, Austria
Email: {fademaj, mtaranet, mrupp}@nt.tuwien.ac.at

***Abstract*—Beamforming and Multiple Input Multiple Output (MIMO) have been identified as key technologies to meet the ever increasing capacity demands in future mobile cellular networks. So far, these features have mainly been investigated in the azimuth dimension, considering one-dimensional antenna arrays. Recently, the 3rd Generation Partnership Project has released a new 3-dimensional (3D) spatial channel model that also accounts for the elevation. It supports two-dimensional antenna arrays and enables to scrutinize concepts such as elevation beamforming and Full Dimension-Multiple Input Multiple Output. However, existing studies have mainly been carried out with commercial tools, thus largely limiting their reproducibility. This paper provides a guideline for the practical implementation of the 3D channel model into existing link- and system level simulation tools. Considering the complexity of the model itself, our main focus is on computational efficiency. We validate our approach with the Vienna LTE-A Downlink System Level Simulator and present simulation examples with various planar antenna arrays and polarization schemes.**

***Index Terms*—3GPP 3D channel model, system level simulations, link level simulation, open source, elevation beamforming, full dimension-MIMO, vertical sectorization, channel coefficient generation**

I. Introduction

Developing realistic channel models is one of the greatest challenges in describing wireless communications. Their quality is crucial for accurately predicting the performance of a wireless cellular system. Channel models can be broadly divided into two categories, *deterministic* and *stochastic*. Deterministic models describe the channel for a *specific* propagation environment between transmitter and receiver. Since this method can be tedious to evaluate and does not allow for general statements in an ensemble of environments, the channel characteristics are often condensed to a statistical description, e.g., the *typical* Power Delay Profile (PDP).

In order to close the gap between the two approaches, 3rd Generation Partnership Project (3GPP) introduced the Spatial Channel Model (SCM) [1]. This model represents scatterers through statistical parameters without being physically positioned. It is also known as a *geometric stochastic* model and separately defines *large scale parameters* (e.g., shadow fading, delay spread and angular spreads) as well as *small scale parameters* (e.g., delays, cluster powers, and arrival- and departure angles). Both parameter sets are randomly drawn from tabulated distributions. The large scale parameters incorporate the geometric positions of the Base Stations (BSs) and the Users (UEs), and are used to parameterize the statistics of the small scale parameters. Then, the channel behavior is defined based on the PDP and the Angular Profile (AP).

978-1-4673-6540-6/15/$31.00 © 2015 IEEE

The SCM model in [1] includes six different scenarios, each of them representing a unique environment. Since it was targeted for a bandwidth of only $5\,\mathrm{MHz}$, and a carrier frequency of $2\,\mathrm{GHz}$, 3GPP extended this model to the so-called Spatial Channel Model Extended (SCME). It follows the same procedure as SCM but supports bandwidths of up to $100\,\mathrm{MHz}$ and a frequency range of $2 - 6\,\mathrm{GHz}$. In the course of the Wireless World Initiative New Radio (WINNER) projects, the model was extended for 15 different scenarios [2, 3], including urban-, rural- and moving environments. The WINNER model is also recommended as a baseline for the evaluation of radio interface technologies in the International Telecommunication Union - Radiocommunication Sector (ITU-R) [4].

All models presented above are limited to the azimuth dimension. Thus, when it comes to describing Multiple Input Multiple Output (MIMO) systems, only linear antenna arrays in the horizontal direction are supported. As interest in 3-dimensional (3D) beamforming is greatly increasing, enabling concepts such as Full Dimension (FD)-MIMO and vertical sectorization, modeling the elevation direction is becoming indispensable. Recently, 3GPP introduced a new 3D SCM for LTE-Advanced (LTE-A) [5].

Yet, only few simulation studies, including reports from the 3GPP TSG RAN WG1 meetings, have been published that claim the practical implementation of the model [6, 7]. However, the employed tools are mainly developed by network operators and vendors, and thus typically intended for commercial use. The authors believe that *open access* is a key prerequisite for reproducible simulation studies. This paper is the first to provide a guideline for the practical implementation of the model. The MATLAB source code is openly available for download on our webpage www.nt.tuwien.ac.at/vienna-lte-a-simulators under an academic, non-commerical use license. It is provided as a stand-alone package that is directly applicable for system level simulation tools and can straightforwardly be ported to link level.

This contribution outlines as follows. The guideline for a computationally efficient implementation of the 3GPP 3D

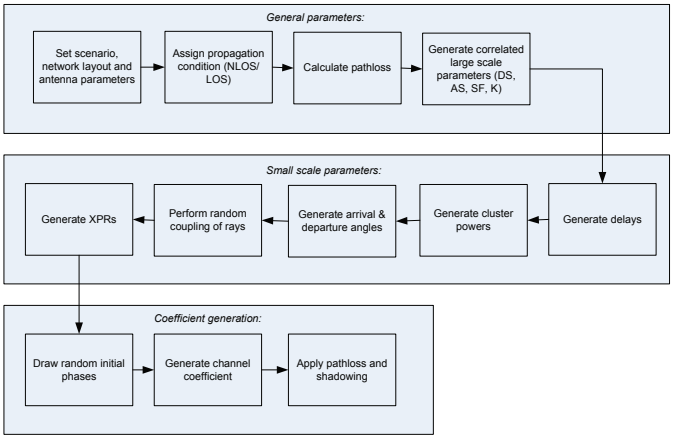

Fig. 1: Procedure for generating coefficients of fast fading MIMO channel as defined in [5].

channel model is presented in Section II. In Section III, the implementation is validated against results from the 3GPP standard with the Vienna LTE-A Downlink System Level Simulator. While 3GPP provides the specifications for the new 3D channel model, parametrization examples for specific test cases and transmission scenarios currently seem to be missing (April 2015). We provide a few parameter sets within this paper that we experienced as typical in the past. Moreover, simulation results for various planar antenna array patterns and polarization schemes are provided. Section IV outlines new opportunities for investigations and Section V concludes the work.

II. 3D Channel Model in System Level Simulator

In this section, we describe the necessary steps to integrate the 3D channel model into an existing simulation tool. The target is to compute a $N_{\mathrm{Rx}} \times N_{\mathrm{Tx}}$ MIMO-channel matrix $\mathbf{H}(t,f)$ for each sampling point on the time-frequency grid[1], where N_{Tx} and N_{Rx} denote the number of transmit- and receive antenna *ports*, respectively.

In the 3D channel model, the channel coefficients are largely dependent on the UE location in the 3D space and, thus, have to be calculated *at runtime*. Hence, the challenge is to perform computationally intensive tasks off-line or on demand, whenever possible. We will follow the stepwise procedure[2] as specified in [5, Sec. 7.3] and illustrated in Figure 1, and explain its expedient partition for implementation.

[GP] The first step is to generate the *general parameters*. It starts with setting the network layout, the scenario environment and the antenna array parameters (*Step 1*). Currently, the standard specifies two scenarios, 3D-Urban Macro cell (UMa) and 3D-Urban Micro cell (UMi), and various planar antenna array structures, defining the location and polarization of each antenna element, as well as the element-to-port mapping. The next steps are to assign the propagation conditions (*Step 2*), i.e., either Line of Sight (LOS) or Non-Line of Sight (NLOS), calculate the experienced path loss (*Step 3*) and generate the large scale parameters[3] (*Step 4*) *for each 3D location* within the region of interest. These tasks can be performed off-line, i.e., before entering the actual simulation loop. Similar to the generation of the shadow fading, they have to be carried out only *once per eNodeB site*.

[SSP] The next step is to generate *small scale parameters*. In the 3D channel model, channel coefficients $H_{u,s,n}(t,f)$ are determined individually for each cluster n and each receiver- and transmitter *antenna element* pair $\{u,s\}$, respectively. The calculation of $H_{u,s,n}(t,f)$ requires to generate delays (*Step 5*), cluster powers (*Step 6*) as well as arrival- and departure angles for both azimuth and elevation (*Step 7*). After coupling the rays within a cluster (*Step 8*), Cross Polarization Power Ratios (XPRs) and random initial phases are drawn (*Step 9 and 10*). Together with the calculation of the spherical unit vectors and the Doppler frequency component (both *Step 11*), all parameters mentioned above are commonly applied to each antenna element pair $\{u,s\}$ and thus have to be determined only *once* per antenna array and physical RB. The latter accounts for the frequency-selectivity of the channel.

[CG] The final channel matrix $\mathbf{H}(t,f)$ is obtained by first aggregating the channel coefficients of all clusters n of an individual pair $\{u,s\}$, i.e., $H_{u,s}(t,f) = \sum_n H_{u,s,n}(t,f)$, and then combining the cumulative channels according to the antenna element-to-port mapping, i.e., $[\mathbf{H}(t,f)]_{m,n} = \sum_{u\in\mathcal{P}_m} \omega_u \sum_{s\in\mathcal{P}_n} \omega_s H_{u,s}(t,f)$, where $\mathcal{P}_m$ and $\mathcal{P}_n$ denote the sets of antenna elements that belong to receive antenna port m and transmit antenna port n, and ω_u and ω_s are complex weights that account for phase shifts as applied for static beamforming (e.g., electrical downtilting), respectively.

Considering a UE with a fixed location in the 3D space, ***[SSP]*** and ***[CG]*** have to be carried out only in the first time instant of the simulation. Afterwards, the channel will remain static over time (no Doppler). If the UE moves at a certain speed, represented by the vector $\mathbf{v} \in \mathbb{R}^3$, in principle, ***[SSP]*** and ***[CG]*** would have to be performed at runtime in each time instant of the simulation. This also implies the generation of new clusters and random initial phases, i.e., a complete change of the multi-path propagation environment. Thus, it is considered reasonable from a physical perspective (see, e.g., [3]) as well as in view of computational complexity to partition the scenario into equally sized cubes. As long as the UE resides within the same cube, it is assumed to experience the same path loss, shadow fading, propagation conditions (LOS/NLOS) and large scale parameters, as generated in ***[GP]***. Then, ***[SSP]*** has to be carried out only once at the beginning of the simulation and each time the UE transfers to another

[1]On link level, channel realizations are typically calculated per OFDM symbol and LTE-A subcarrier [8]. On system level, they are commonly generated per physical Resource Block (RB) [9].

[2]The steps are denoted as '*Step N*' with $N \in \{1,..,12\}$.

[3]The vector of large scale parameters incorporates shadow-fading, the Ricean K-factor (only in the LOS case), delay-spread, azimuth angle spread of departure- and arrival, as well as zenith angle spread of departure- and arrival. The latter have become available not until the introduction of the 3D channel model.

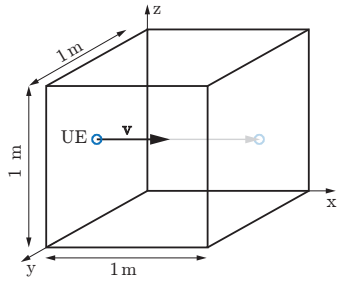

Fig. 2: UE travels through cube with an edge length of 1 m.

cube[4]. Within a cube, channel variations are caused by the slightly changing angles of arrival and departure (and thus the antenna element field patterns) as well as the phase shift due to the Doppler. They can be incorporated into ***[CG]***, thus yielding the only variable components that have to be recalculated in each time instant of the simulation.

III. Calibration and Simulation Examples

Following the steps in Section II, we incorporated the 3D channel model in the Vienna LTE-A Downlink System Level Simulator (current version v1.8r1375) [9]. The simulator is implemented in object-oriented MATLAB and is made openly available for download under an academic, non-commercial use license. It is built according to the commonly employed structure for system level simulation tools (see, e.g., in [10, 11]), as illustrated in Figure 3, thus serving as a representative example. Its centerpiece is the *link abstraction model* that specifies the interaction between link- and system level simulations [9, 10]. This structure is expected to persist in simulation tools for the fifth generation of mobile cellular networks (5G) [11]. The enhancements that were necessary to enable the 3D channel model are depicted by the boxes shaded in gray at the top of the figure.

A. Calibration

For calibration purposes, we carry out simulations with the setup as specified in [5, Table 8.2-2]. The setup is summarized in Table I. Two scenarios, 3D-UMa and 3D-UMi are investigated. They represent typical urban macro-cell- and micro-cell environments. While the former consider a BS height of $(25\,\mathrm{m})$, surpassing the surrounding buildings, the latter specify a BS height of $(10\,\mathrm{m})$, thus lying below the rooftop level. Moreover, all parameters for computing path loss, shadow fading, large scale parameters and small scale fading are specifically defined for each scenario. Both 3D-UMa and 3D-UMi are assumed to be densely populated with buildings and take into account both indoor- and outdoor UEs. Figure 4 depicts the obtained statistics of the large scale parameters as generated for each UE based on *Step 4* (conf. Section II).

[4]Assuming a spatial resolution of 1 m and a temporal resolution of 1 ms, referring to the length of one LTE sub-frame, also denoted as *Transmission Time Interval (TTI)*, a UE moving at $\mathbf{v} = [27.78, 0, 0]\,\mathrm{m/s}$ requires 36 ms to travel from one face of the cube to the other, as indicated in Figure 2. In this case, ***[SSP]*** is called every 36 sub-frames.

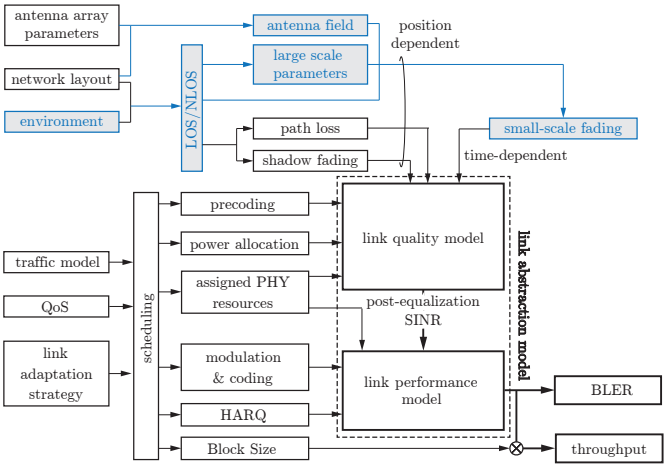

Fig. 3: Enhanced link abstraction model for enabling 3D channel modeling.

TABLE I: Simulation parameters for calibration as referred from [5].

Parameter	Value
Carrier frequency	2 GHz
LTE bandwidth	10 MHz
Macro-site deployment	hexagonal grid
Scenarios	3D-UMa, 3D-UMi
BS antenna height (UMa)	25 m
BS antenna height (UMi)	10 m
BS antenna configuration	$N_{\mathrm{Tx}} = 4$
UE antenna configuration	$N_{\mathrm{Rx}} = 2$
Polarized antenna modeling	Model 2 [5]
BS antenna polarization	X-pol $(+/-45^\circ)$
UE antenna polarization	X-pol $(0/+90^\circ)$
Antenna elements per port	$M = 10$
Vertical antenna element spacing	$\lambda/2$
Horizontal antenna element spacing	$\lambda/2$
Maximum antenna element gain	8 dBi
Electrical downtilt	12°
UE distribution	uniform in cell [5]

The parameters incorporate the spatial-correlation among UEs served by the same eNodeB as well as cross-correlations among the parameters themselves. In accordance with the results in [12], the distributions show similar characteristics for 3D-UMa and 3D-UMi. It is further observed that they show a good agreement with results from [5] (dash-dotted curves) that were obtained by averaging over 21 sources[5].

B. Simulation Examples

In this section we consider a network with seven macro sites, each employing three eNodeBs, and simulate 50 randomly distributed UEs per eNodeB sector. Our goal is to compare the throughput performance for various antenna array configurations at the eNodeB. We consider four antenna ports, i.e., $N_{\mathrm{Tx}} = 4$, and compare linear and cross-polarized antenna

[5]In the calibration part of [5], results are only provided for the zenith angle spreads.

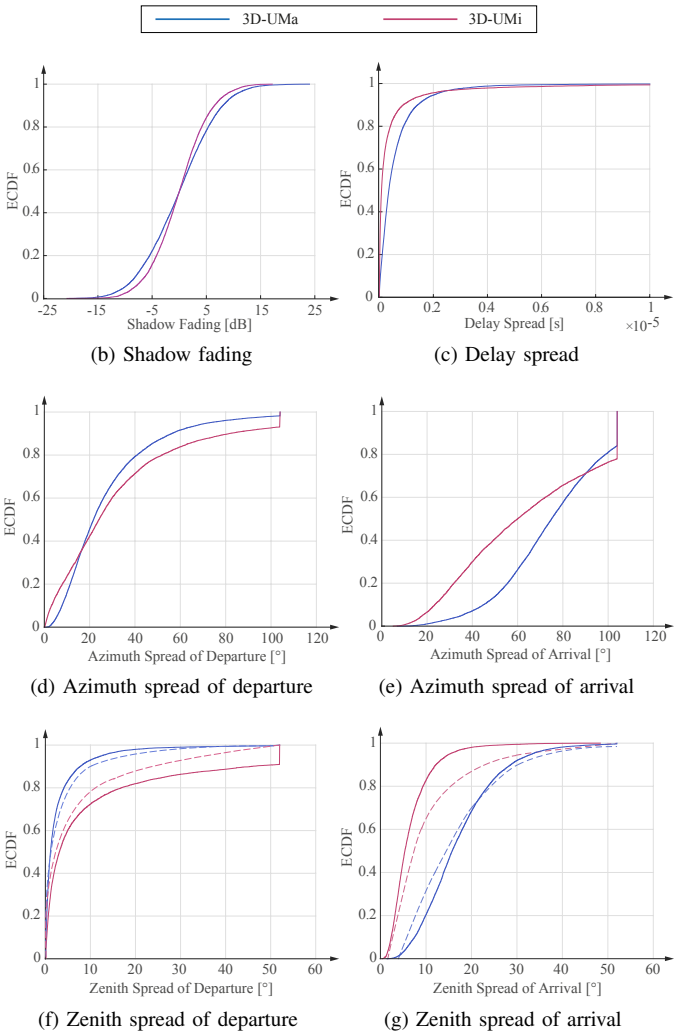

(b) Shadow fading (c) Delay spread

(d) Azimuth spread of departure (e) Azimuth spread of arrival

(f) Zenith spread of departure (g) Zenith spread of arrival

Fig. 4: Large scale parameter statistics. Solid lines refer to results 3D-UMa and 3D-UMi scenario. Dashed curves denote reference results from [5].

element arrangements[6], further denoted as *Config 1* and *Config 2*, respectively. Secondly, we vary the antenna array geometry, assuming setups with $M = 2$ and $M = 10$ antenna elements per antenna port, as indicated in Figure 5. The UEs are equipped with a single linearly polarized antenna element that is attached to a single antenna port. The simulation setup is summarized in Table II.

Figure 6 depicts simulation results in terms of average UE throughput statistics. It is observed that, remarkably, *Config1* achieves an almost two-times higher throughput than *Config2*, just by employing the same polarization direction as the UE. Moreover, it is seen that using $M = 2$ instead of $M = 10$ antenna elements per column decreases the performance. This is mainly caused by the fact that with $M = 10$ elements in the vertical direction, a sharper static beam can be achieved by

[6]The slant angle is incorporated by using *Polarization Model-2* from [5, Sec. 7.1.1], as this model yields the best agreement with results from measurements [13].

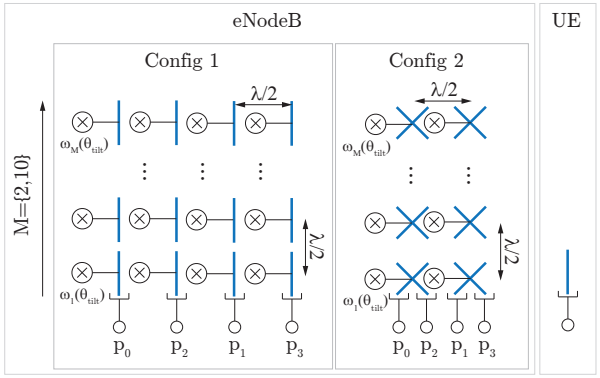

Fig. 5: Antenna array configurations. The antenna ports are denoted as p_i with $i \in \{1, \ldots, 4\}$, and ω_j, $j \in \{1, \ldots, M\}$ are the phase shifts for static beamforming (e.g., electrical downtilting).

TABLE II: Simulation setup

Parameter	Value
Carrier frequency	2 GHz
LTE bandwidth	10 MHz
Macro-site deployment	hexagonal grid
Scenario	3D-UMa
Inter-site distance	500 m
eNodeB transmit power	46 dBm
Polarized antenna modeling	model 2 [5, Sec. 7.1.1]
Maximum antenna element gain	8 dBi
Vertical antenna element spacing	$\lambda/2$
Horizontal antenna element spacing	$\lambda/2$
Electrical downtilt	12°
Number of UEs per cell	50
UE speed	3km/h
Receiver type	zero forcing
Channel knowledge	perfect
Feedback delay	3 TTIs
Noise power density	−174 dBm/Hz
LTE transmission mode	4
Scheduler	proportional fair
Traffic model	full buffer
Simulation length	50 TTIs
Number of simulation runs	20

the electrical down-tilting. The figure further shows separate statistics for LOS- and NLOS UEs for each scenario. It is seen that UEs in LOS achieve a considerably better throughput performance than in NLOS. Remarkably, the width of the gap depends on the polarization scheme and the number of antenna elements per column.

IV. New Opportunities

The integration of the 3D channel model into existing link- and system level simulation tools paves the way for more advanced studies on the performance of a mobile cellular system in realistic environments. Existing channel models only supported linear antenna arrays in the azimuth. With the introduction of the third dimension, not only higher-order MIMO schemes but also higher number of antenna elements per antenna array can be investigated. Currently, the

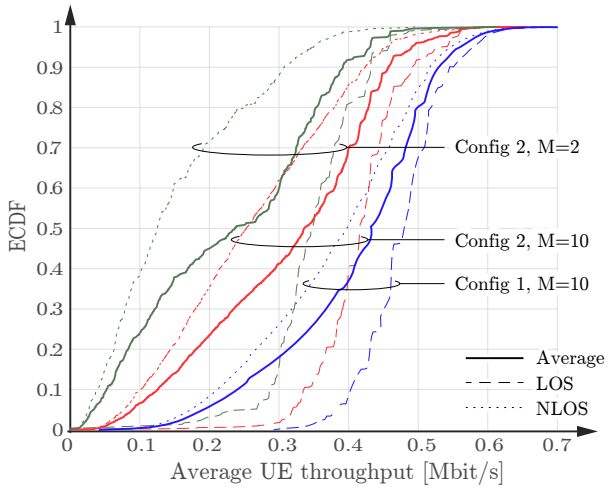

Fig. 6: Average UE throughput [Mbit/s] ECDF curves for various antenna polarization schemes and antenna array structures. Solid lines depict typical throughput. Dashed and dotted lines show performance as achieved by LOS and NLOS UEs.

3GPP LTE-A standard supports up to eight antenna ports. However, current trends aim at 100 and more antenna ports per eNodeB [14]. A main enabler for this so called *massive MIMO* approach will be the adoption of higher carrier frequencies, also termed *millimeter-wave communication*, as it enables to considerably decrease the size of the antenna arrays. On the one hand, this may lead to higher complexity of the hardware, larger energy consumption and a greater demand for signal processing capabilities. On the other hand, it will enable a much more accurate bundling of energy towards the intended receiver, which is a key prerequisite for aggressive frequency reuse. In dense urban environments, where UEs move in three dimension (consider, e.g., shopping malls, skyscrapers, and more) it is conceivable that the spectral efficiency per unit sphere might replace the area spectral efficiency as a figure of merit. Other important use cases are scenarios with high user mobility, as the number of commuters is expected to increase substantially. People have become used to services following them wherever they travel. Mobile cellular access has even become a key argument to choose the means of transportation. Sharp, steerable beams might be an expedient solution to this issue, as they could follow a vehicle along its path.

V. Conclusion

This paper presented a guideline for the practical implementation of the 3GPP 3D channel model into existing link- and system level simulation tools. We met the challenge of calculating the channel coefficients at simulation runtime by carefully partitioning the step-wise procedure as proposed by the 3GPP. We demonstrated the validity of our approach by integrating it into the Vienna LTE-A Downlink System Level Simulator. The obtained large scale parameters statistics showed a good agreement with the results which are provided by the 3GPP for calibration. We carried out example simulations with various antenna array setups and observed a strong impact of the antenna polarization on the typical UE performance. We completed the work with an elaboration on new opportunities that became possible with the 3D channel model. Our hope is to inspire researches and developers of link- and system level simulation tools to further elaborate on these topics by directly applying or reusing our implementation approach.

Acknowledgments

This work has been funded by the Christian Doppler Laboratory for Wireless Technologies for Sustainable Mobility, the A1 Telekom Austria AG, and the KATHREIN-Werke KG. The financial support by the Federal Ministry of Economy, Family and Youth and the National Foundation for Research, Technology and Development is gratefully acknowledged.

References

[1] 3rd Generation Partnership Project (3GPP), "Spatial channel model for Multiple Input Multiple Output (MIMO) simulations," 3rd Generation Partnership Project (3GPP), TR 36.996, Sept. 2003.

[2] WINNER I WP5, "Final report on link level and system level channel models," *IST-2003-507581 WINNER I Deliverable D5.4*, Nov. 2005.

[3] WINNER II WP1, "WINNER II channel models," *IST-4-027756 WINNER II Deliverable D1.1.2*, Sept. 2007.

[4] M. ITU-R, "Guidelines for evaluation of radio interface technologies for IMT-Advanced," *Report*, Dec. 2009.

[5] 3rd Generation Partnership Project (3GPP), "Study on 3D channel model for LTE," 3rd Generation Partnership Project (3GPP), TR 36.873, Sept. 2014.

[6] A. Kammoun, H. Khanfir, Z. Altman, M. Debbah, and M. Kamoun, "Preliminary results on 3D channel modeling: From theory to standardization," *IEEE Journal on Selected Areas in Communications*, vol. 32, no. 6, pp. 1219–1229, June 2014.

[7] Z. Hu, R. Liu, S. Kang, X. Su, and J. Xu, "Work in progress: 3D beamforming methods with user-specific elevation beamfoming," in *International Conference on Communications and Networking in China (CHINACOM)*, Aug. 2014, pp. 383–386.

[8] S. Schwarz, J. Ikuno, M. Simko, M. Taranetz, Q. Wang, and M. Rupp, "Pushing the limits of LTE: A survey on research enhancing the standard," *IEEE Access*, vol. 1, pp. 51–62, 2013.

[9] M. Taranetz, T. Blazek, T. Kropfreiter, M. Müller, S. Schwarz, and M. Rupp, "Runtime precoding: Enabling multipoint transmission in LTE-Advanced system level simulations," *accepted for revision in IEEE Access*, 2015.

[10] S. Ahmadi, *LTE-Advanced: A Practical Systems Approach to Understanding 3GPP LTE Releases 10 and 11 Radio Access Technologies*, ser. ITPro collection. Elsevier Science, 2013.

[11] Y. Wang, J. Xu, and L. Jiang, "Challenges of system-level simulations and performance evaluation for 5G wireless networks," *IEEE Access*, vol. 2, pp. 1553–1561, 2014.

[12] 3GPP TSG RAN WG-1, "R1-140048: Phase 2 calibration results for 3D channel model," 3rd Generation Partnership Project (3GPP), Tech. Rep., Feb. 2014.

[13] ——, "R1-140765: Polarized antenna modeling," 3rd Generation Partnership Project (3GPP), Tech. Rep., Feb. 2014.

[14] F. Rusek, D. Persson, B. K. Lau, E. Larsson, T. Marzetta, O. Edfors, and F. Tufvesson, "Scaling up MIMO: Opportunities and challenges with very large arrays," *IEEE Signal Processing Magazine*, vol. 30, no. 1, pp. 40–60, Jan. 2013.